Chemical Physics Letters 609 (2014) 161–166

Contents lists available at ScienceDirect

Chemical Physics Letters

journal homepage: www.elsevier.com/locate/cplett

Control of band structure of van der Waals heterostructures: Silicene on ultrathin silicon nanosheets

Shuang Li, Yifeng Wu, Wei Liu*, Yonghao Zhao*

Nano Structural Materials Center, Nanjing University of Science and Technology, Nanjing 210094, Jiangsu, PR China

A R T I C L E I N F O

Article history:
Received 6 May 2014
In final form 24 June 2014
Available online 1 July 2014

A B S T R A C T

The geometric and electronic properties of silicene on doping ultrathin silicon nanosheet were performed using dispersion-corrected density-functional theory. The results show that the substrates modify the electronic properties of silicene due to the difference of charge population between the two sublattices. A sizable band gap is created at the Dirac point, which could be widened by bias voltage. It is theorized that the hetero-structures could provide a viable route to silicene-based electronic devices.

Silicene exhibits fascinating electronic properties, for example, it has relativistic Dirac fermions [1–4], and has strong spin–orbit coupling for potential topological insulator candidates [5]. More importantly, these specific electronic properties are expected to be experimentally realized via silicon-based nanotechnology in the near future [6]. In a silicene structure, hexagonal mesh of silicon atoms are ordered in a low-buckled structure [7–8], and this structural flexibility may give rise to altered electronic properties [9]. Recent experimental studies have revealed silicene monolayer honeycomb structures could be achieved experimentally on Ag(111) [10–11], $ZrB_2(0001)$ [12], (2×1) reconstructed Au(110) [13], and Ir(111) surfaces [14]. The above successful synthesis of silicene ribbons and sheets takes a further step towards the applications of silicene as a nanoscale device. However, the absence of a band gap around the Fermi level in silicene limits its applications. Therefore, the urgent troublesome problems need to be solved in this field is to developing methods to functionally tailor band gap size.

Van der Waals (vdW) hetero-structure has recently been paid significant attentions [15]. As we know, hetero-structures of graphene on hexagonal boron nitride (h-BN) have promised a crucial advantage over graphene for broader applications, such as graphene/BN multilayer transistors [16–18]. Very recent work has demonstrated that the hetero-structures could open a sizable band gap through designing suitable substrates [19–21]. Besides that, studies have been carried out to address the effects of substrate on the electronic properties of silicene. For example, by using the ZnS(0001) as a substrate, Houssa et al. [19] achieved a band gap of 0.7 eV and found that the ZnS substrate strongly interacts with the silicene. In contrast, the band gap cannot be opened when the silicene is located at the substrate containing h-BN and SiC(0001) [20]. Gao et al. [21] studied silicene on twelve different substrates with band gap ranging from 4 to 181 meV. In addition, Ding et al. [22] reported that the band gap of silicene/GaS nanosheets can be modulated by strain and external electric field. The involvement of substrates is indeed an effective way to open a band bap in silicene. Nevertheless, some important issues remain largely unexplored, for example, how to choose a suitable substrate; what is the mechanism to open the band gap; and how to control the width of the band gap.

The growth of silicene on semiconductor or insulating substrates is required for its potential applications in nanoelectronic devices [19–20]. As a substrate, functional ultrathin silicon nanosheets are suitable choice. Both experimental and theoretical studies have demonstrated the feasibility of fabricating such nanosheets [23,24]. These wide-gap nanostructures process a layered structure, which is very similar to that of silicene [21,23–25]. The lattice mismatch of silicene with these nanostructures are small, and the two atoms in the unit cell are chemically inequivalent. Therefore, it would be of great importance to understand how functional ultrathin silicon nanosheets affect the atomic and electronic structures of silicene.

In this Letter, we carried out density-functional theory (DFT) calculations to study the detailed geometric and electronic properties of silicene on the substrates of hydrogen (or fluorine) functional and phosphorus substitutional doping ultrathin silicon nanosheets. The H-saturated silicon sheets (silicane) have been synthesized in the form of layers polysilane since 1993 [26–27], and many theoretical studies have focused on the silicane [23–24]. Due to the fact that vdW interactions play an essential role in hybrid layered materials, the vdW-inclusive method DFT-D2 of Grimme [28] is utilized in our calculations. The computations employed an all-electron method [29–30], using generalized gradient approximation (GGA) with exchange–correlation potential

---

* Corresponding authors.

E-mail addresses: amweiliu@gmail.com (W. Liu), yhzhao@njust.edu.cn (Y. Zhao).

http://dx.doi.org/10.1016/j.cplett.2014.06.047
0009-2614/

prescribed by Perdew-Burke-Ernzerhof (PBE) [31], as implemented in the DMol^3 package [28–31]. In addition, double numerical plus polarization (DNP) [32] is chosen as the basis set with orbital cutoff of 4.4 Å [33]. The Brillouin zones are sampled by a set of k-points grid ($8 \times 8 \times 1$) according to the Monkhorst–Pack approximation. The convergence tolerance of energy of 1×10^{-6} Ha (1 Ha = 27.21 eV), maximum force of 0.002 Ha/Å, and the maximum displacement of 0.005 Å in the geometry optimization are taken. Periodic boundary condition is used to simulate 2D infinite sheet, and a vacuum width of 30 Å is used in the direction normal to the sheet in order to avoid interactions between image atoms.

A low-buckled silicene with a (2×2) supercell was placed on top of the monolayer sheet (or double-layer structure). Note that we also used (3×3) and (4×4) supercells to check the convergence of our calculated results and confirmed that the (2×2) supercell is large enough for our calculations. Due to the large difference in electronegativity between H atom and F atom, three decorated silicene configurations with H and F atoms (defined as XSiY, where X and Y are H or F) are considered in this study: a fully hydrogenated (HSiH), fully fluorinated (FSiF) silicene, and half-hydrogenated and half-fluorinated silicene with H on one side and F on the other side (HSiF). For the free-standing silicene, our computed lattice constant (3.828 Å) and the optimized Si–Si bond length (2.252 Å) agree well with other theoretical results [8,34].

There are four possible stacking structures for the silicene/silicane (Si/HSiH) systems, which are denoted as AB-1, AB-2, AA-1 and AA-2 [see Figure 1a–d]. Figure 1e shows the cohesive energy of Si/HSiH as a function of interlayer distance l_0 using the DFT-D2 method, which illustrates that the AB-1 stacking is 10–30 meV/atom more stable than the AB-2, AA-1 and AA-2 structures. Correspondingly, the calculated l_0 for the AB-1 structure is significantly shorter than the rest, with the sequence of AB-1 (1.990 Å) < AA-2 (2.749 Å) < AA-1 (2.763 Å) < AB-2 (2.792 Å). The AB-1 structure has a distinctly energy minima at ~2.0 Å, a typical distance for chemisorption [34–36]. The above findings have also been confirmed by the PBE+vdW method [37] (l_0 = 2.066 Å for AB-1).

Although both PBE and DFT-D2 calculations indicate that silicene can stably attach on silicane without any energy barriers (Figure 1f), the pure PBE functional without vdW correction fails to give a stable adsorption state. Specifically, there is no well-defined minimum in the cohesive-energy curve, and the cohesive energy is significantly underestimated compared to the vdW-inclusive results. The formation energy E_f, which describes the binding strength between the pristine silicene and the substrate, is defined as:

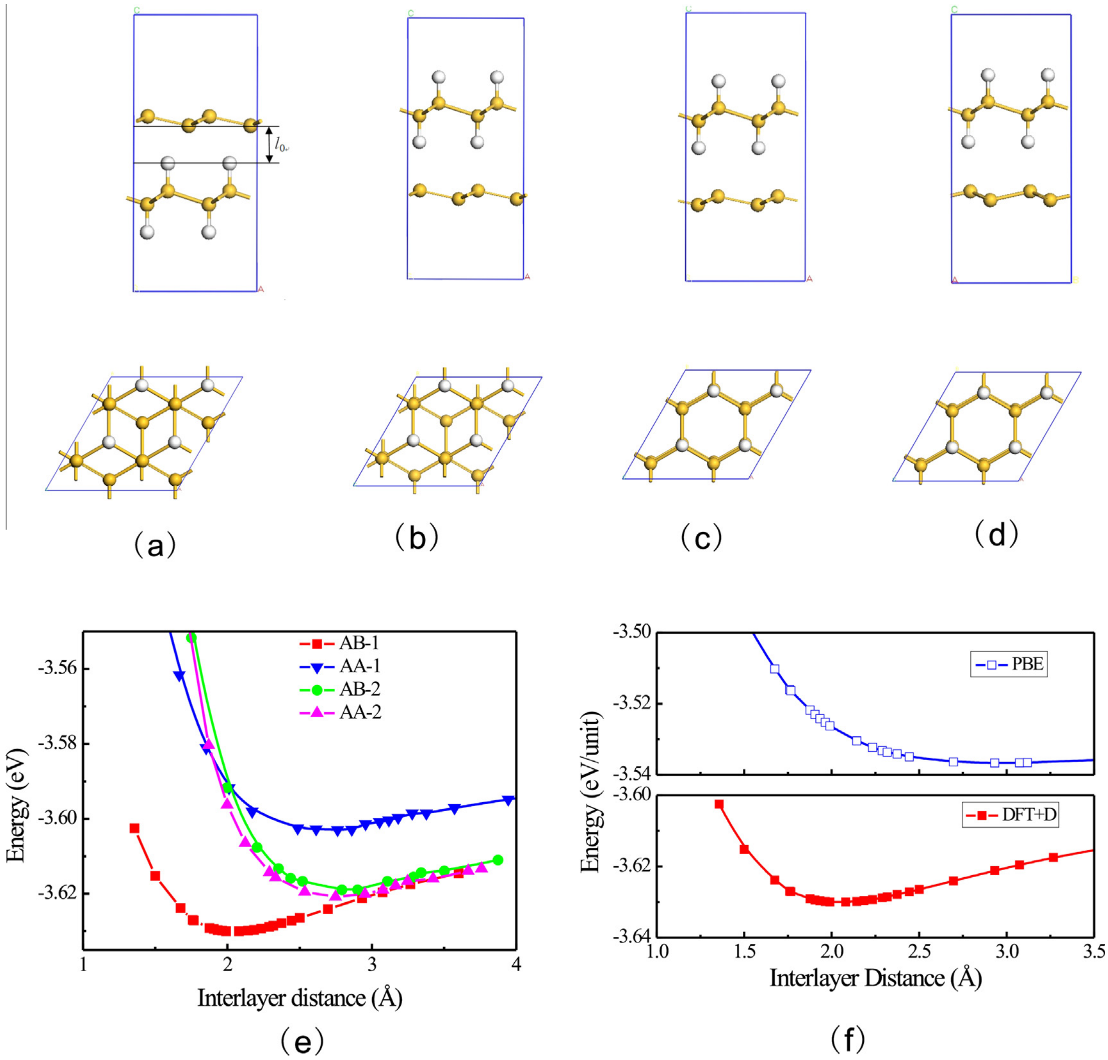

Figure 1. Side (top) and top (bottom) views of four atomic configurations for AB and AA stacked bi-layers of Si/HSiH in a (2×2) supercell, (a) AB-1, (b) AB-2, (c) AA-1 and (d) AA-2. Yellow and white spheres denote Si and H atoms, respectively. (e) Adsorption energy of silicene on silicane as a function of interlayer distance between the two layers. (f) Comparison of the adsorption results of AB-1 using PBE and DFT-D2. (For interpretation of the references to colour in this figure legend, the reader is referred to the web version of this article.)

Table 1
The formation energy E_f (eV) of optimized geometries of silicene on substrate systems by vdW-inclusive method DFT-D2 in four types stacking and PBE exchange-correction functional in AB-1 stacking structure.

	DFT-D2				PBE
	AA-1	AA-2[a]	AB-1	AB-2[b]	AB-1
Si/HSiH	0.344	0.388	0.610	0.357	0.085
Si/FSiF	0.425	–	0.541	0.386	0.136
Si/FSiH	0.343	0.303	0.439	0.301	0.066
Si/HSiF	0.326	0.360	0.615	0.370	0.084
Si/PDL	0.562	–	1.215	1.071	0.328
Si/DLH	0.387	0.452	0.685	0.452	0.082

[a] When the substrate are FSiF and P-DL, the heterostructures in AA-2 stacking are unstable.

[b] AB-1 and AB-2 Si/DLH have the same structure.

$$E_f = (E_{silicene} + E_{sub} - E_{system}) \tag{1}$$

where $E_{silicene}$, E_{sub}, and E_{system} are the cohesive energy of the free standing silicene, the substrate, and the hetero-structure with the same unit cell, respectively. The formation energy for silicene on different substrates with all stacking structures are listed in Table 1, which clearly shows that the AB-1 structure is the most favorable stacking structure. The DFT-D2 formation energy (0.610 eV) for the configuration shown in Figure 1a is significantly larger than the PBE result (0.084 eV) but somehow close to the LDA result (0.729 eV) [21]. It is also notable that the AB-1-Si/HSiH is thermodynamically stable since no imaginary frequency appears from the phonon analysis.

We now study the electronic properties of Si/XSiX structure (X = H and F). Silicene is a zero-gap semimetal, while HSiH and FSiF are insulators with a theoretical band gap of 3.07 and 1.46 eV [38], respectively. To understand the role of layer interactions on the electronic properties of silicene, we computed the band structures of AB-1 type Si/XSiX heterosheets. As shown in Figure 2a and c, the interaction of silicene with H-terminated substrates can open a band gap by 115–139 meV. We find that the major factor inducing band gap is the H-terminated surface, which implies that the heterostructures are identical if the substrate is H-terminated Si (111). It is notable that a very recent paper has shown that the X-terminated Si(111) (X = H, N, F, or Cl) can now be readily obtained in experiments [39].

In contrast, the silicene becomes metallic for the Si/FSiF system, which is readily seen from Figure 2b. Since the conduction band minima (CBM) of F-silicene is lower than the CBM of silicene, upon the interaction of silicene with F-silicene substrate, the Fermi energy of the Si/FHF is lowered as compared to the silicene structure [20]. Hence, the segment of the Dirac cone is well preserved, but the entire Dirac cone is above the Fermi level.

Figure 2a and d illustrate that the band gap is largely dependent on the nature of the stacking of the interfaces. For AA-2-Si/HSiH, there is 27 meV energy gap at the K point, while the gap is 115 meV in the case of AB-1-Si/HSiH. To gain more insights into the phenomenon, we investigated the charge transfer mechanism between silicene and substrates by analyzing the charge density difference, $\Delta\rho$, for interfaces $\Delta\rho$ is defined as,

$$\Delta\rho = \rho_{total} - \rho_{silicene} - \rho_{sub} \tag{2}$$

where ρ_{total}, $\rho_{silicene}$, and ρ_{sub} denote the total charge densities of hetero-structures, free silicene and substrates, respectively. The Si–H bonds of silicane pointing straight to the center of the hexagonal center is referred to as the Si–H/π structure, which induced the charge located in the center of the honeycomb structure [40]. For the AA-2-Si/HSiH structure, the charge located in the Si atoms, while for the AB-1-Si/FSiF structure, the charge transform from silicene to the interface. The Mulliken population analysis (see Table 2) shows that in the AB-1-Si/HSiH structure, the silicon atoms of silicene uniformly possess −0.010 |e| of charge and in the AA-1-Si/HSiH the silicon atoms of silicene uniformly possess −0.003 |e| of charge. In contrast, in the AB-1-Si/FSiF structure, the silicon atoms of silicene uniformly carry 0.033 |e| of charge, the considerable redistribution of electron density occurs in AB-1-Si/FSiF structure.

The charge populations of any two neighboring silicon atoms different ($|e_1 - e_2|$) may be the major reason to open a larger E_g [21–22]. The superposition of an external electric filed F would significantly amplify the charge distribution. Besides that, Lu's group [41] reported that the band gap of silence increase linearly with the

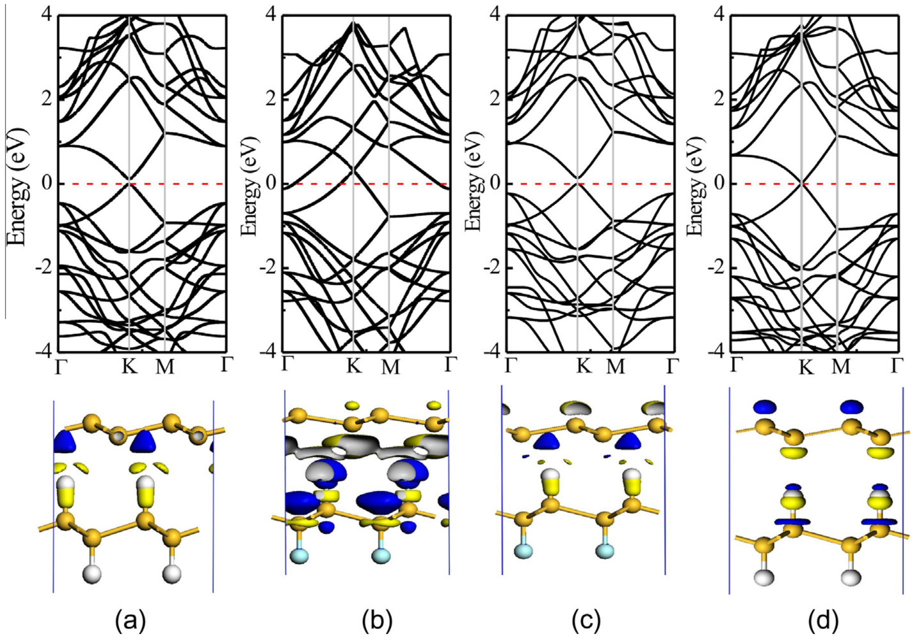

Figure 2. Electron band structures and the valence charge density distribution of bi-layers of Si/XSiX hetero-structures (a) AB-1-Si/HSiH, (b) AB-1-Si/FSiF, (c) AB-1-Si/HSiF, and (d) AA-2-Si/HSiH. The dot lines are Fermi level. The yellow and blue isosurfaces correspond to charge densities of 0.002 and −0.002 |e|/Å^3, respectively. (For interpretation of the references to colour in this figure legend, the reader is referred to the web version of this article.)

Table 2
Detailed electronic information for silicene/substrates by DFT with the vdW-inclusive DFT-D2 method: $|e_1 - e_2|$ (e), Q (e) and E_g (meV) stand for the difference of Mulliken population for 1, 2 sublattices in silicene, total charge population and band energy, respectively.

		$\|e_1 - e_2\|$	Q	E_g
Si/HSiH	AB-1	0.132	−0.010	115
	AA-2	0.023	−0.003	27
Si/HSiF	AB-1	0.154	−0.120	139
Si/FSiH	AB-1	0.058	0.020	Metallic
Si/FSiF	AB-1	0.041	0.033	Metallic

vertical F. As such, one could expect that external F would significantly modify the band gap of hetero-structures. To test the above hypothesis, we superimposed external electric fields into these systems, either along the z axial (positive) or reverse direction (negative). Figure 3a shows the variation of E_g as a function of the imposing F, which clearly shows that the E_g values of the Si/HSiH structure can be indeed turned by electric field. Take the Si/HSiH structure as an example, the band gap decreases monotonously with increasing electric field when $F > 0.01$ V/Å. However, when $0 < F < 0.01$ V/Å a step appears and the band gap varies slightly with the field. The band gap increases linearly with increasing $|F|$ when $-0.06 < F < -0.01$ V/Å. Figure 3b shows the band gap of Si/HSiH under $F = -0.15$ V/Å. We also notice that the band gap changes from direct gap at K point to indirect gap at Γ point, when $F > -0.13$ V/Å.

We also studied the change of band gap with F for silicene on the ultrathin double Si with hydrogenation (DL-H) as substrates [23]. As shown in Figure 4a, the step is located between −0.016 and 0.01 V/Å, presumably because the external field needs to overcome the intrinsic electric field. When F is smaller than −0.10 V/Å, the band gap also changes to indirect one. The band gap of this hetero-structure is stable between −0.016 and 0.01 V/Å, when $F > 0.01$ V/Å it changes to metallic, when $F < -0.016$, the band gap increases linearly with increasing $|F|$.

We have also studied the strain modulated band structure for the Si/DL-H hybrid structure. As shown in Figure 4b, the band gap is sensitive to the in-plane strains, the strains are applied to Si/DL-H hybrid structure by changing the lattices as $\varepsilon = (a - a_0)/a_0$, where a (a_0) is the lattice constant under the strain (equilibrium) condition. The band gap decreases with increasing tension, whereas increasing first and then decreasing with compression. When $-0.013 < \varepsilon < 0.025$, the bang gap changes almost linearly with the strain, ranging from 113 to 169 meV.

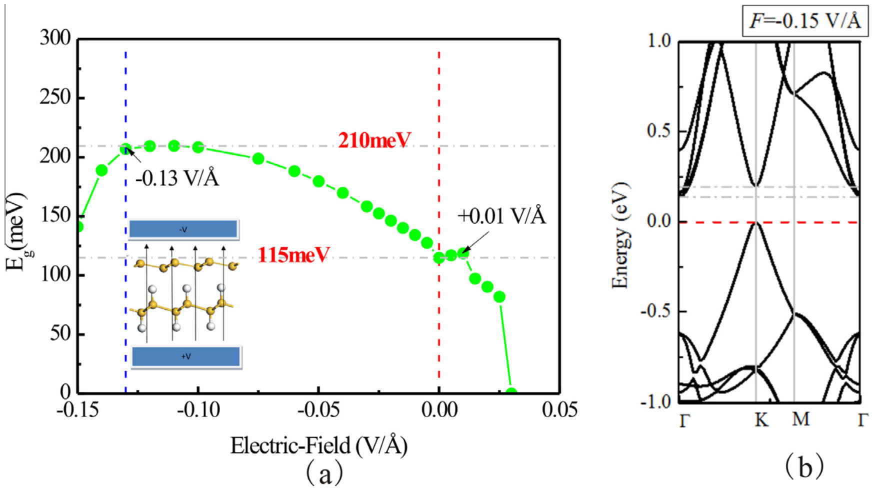

Figure 3. (a) The variation of band gap as a function of external electric field, and (b) the band structure of silicene/silicane under $F = -0.15$ V/Å.

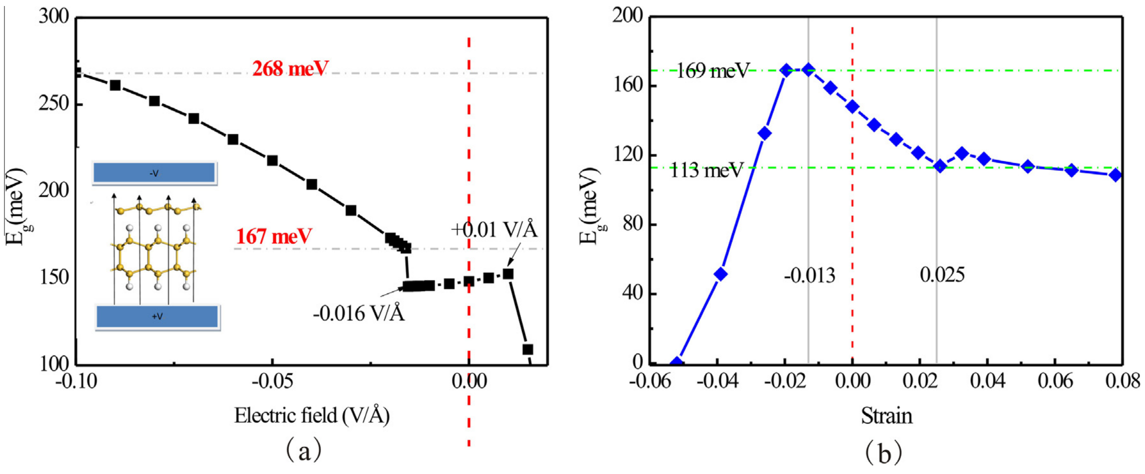

Figure 4. The variation of band gap of Si/DL-H as a function of the electric field intensity (a) and the strain (b).

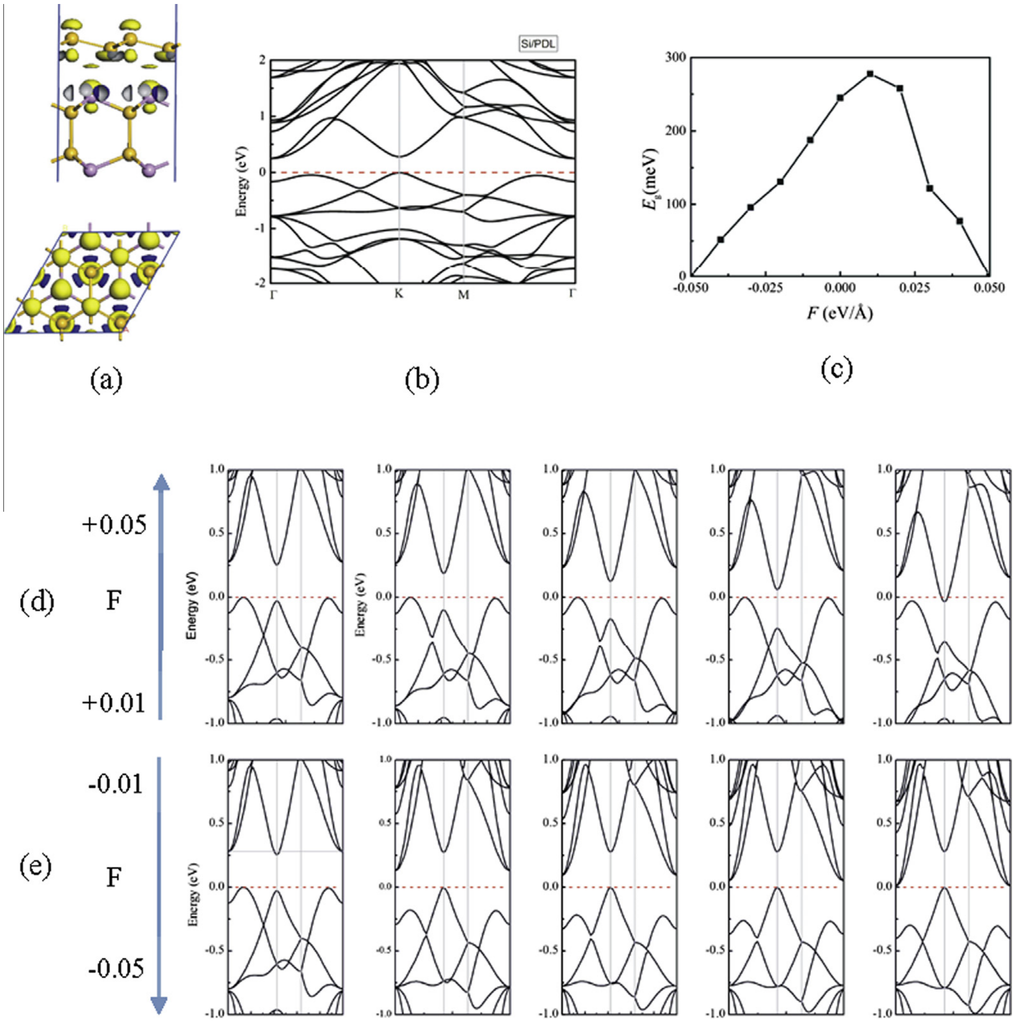

Figure 5. (a) Side, top view valence charge density distribution of bi-layers of Si/P-DL heterostructure, the yellow and blue isosurfaces correspond to charge densities of 0.004 and −0.004 $|e|/Å^3$ respectively; (b) electron band structures of Si/P-DL heterostructure; (c) the variation of band gap as a function of *F*; (d) the band structures of Si/P-DL when *F* vary from +0.01 eV/Å to +0.05 eV/Å; (e) the band structures of Si/P-DL when *F* vary from −0.01 eV/Å to −0.05 eV/Å.

Although imposing *F* works well for opening the band gap of silicene, some more polarizable atoms, such as P, cannot achieve this goal. We used P-DL (see Figure 5a) as substrate, the P-DL structure has an indirect band gap of around 1.5 eV [23], the Si/P-DL heterostructure is also a semiconductors with an indirect gap about 224 meV. The band structure of this hetero-structure has been given in Figure 5b. As illustrated in Figure 5c, the Si/P-DL structure changes from semiconductor to metallic when $|F| > 0.05$ V/Å, which is presumably because the large amount of charge transfer vanishes the band gap of the heterostructure. In addition, the CBM and VBM in K point decrease with *F* increases along the *z* axial (see Figure 5d and e). Therefore, the band gap of Si/P-DL increases first and then decreases. In addition, with increasing *F* reverse *z* axial the CBM at Γ point and VBM between Γ and K point decreases, the band gap of Si/P-DL decreases monotonously.

Conclusion

In summary, using first-principles calculations, we studied the electronic structure of various hetero-structures of silicene with chemical functional silicon ultrathin films. We have demonstrated that the inter-layer weak interactions strongly affect the atomic and electronic structures of the hetero-structures. The Si/DL-H structures are expected to be a proper substrate for silicene: the silicene layer remains simple buckling structure, and also retains the characteristic Dirac-like band features, making them promising 2D semiconductors instead of zero-gap semimetals. Due to the interface charge redistribution, a sizable gap is opened at the Dirac point, which can be further modulated by external electric fields and strains in these hybrid interfaces.

Acknowledgements

The Project Sponsored by the Scientific Research Foundation for the Returned Overseas Chinese Scholars, State Education Ministry. Project supported by the Natural Science Foundation of Jiangsu Province, China (Grant No. BK 20130752).

References

[1] B. Lakmi, H. Oughaddou, H. Enriquez, A. Kara, S. Vizzini, B. Ealet, B. Aufray, Appl. Phys. Lett. 97 (2010) 223109.
[2] D. Chiappe, C. Grazianetti, G. Tallarida, M. Fanciulli, A. Molle, Adv. Mater. 24 (37) (2012) 5088.
[3] L. Pan, H.J. Liu, Y.W. Wen, X.J. Tan, H.Y. Lu, J. Shi, X.F. Tang, Phys. Lett. A 375 (2011) 614.
[4] L. Chen et al., Phys. Rev. Lett. 109 (2012) 056804.
[5] P. De Padova et al., Appl. Phys. Lett. 96 (2012) 261905.
[6] C.C. Liu, W. Feng, Y. Yao, Phys. Rev. Lett. 107 (2011) 076802.
[7] Y. Ding, J. Ni, Appl. Phys. Lett. 95 (8) (2009) 083115.

[8] S. Cahangirov, M. Topsakal, M. Akturk, H. Sahin, S. Ciraci, Phys. Rev. Lett. 102 (2009) 236804.
[9] T.P. Kaloni, Y.C. Cheng, U. Schwingenschlögl, J. Appl. Phys. 113 (2013) 104305.
[10] P. Vogt et al., Phys. Rev. Lett. 108 (2012) 155501.
[11] B.J. Feng et al., Nano Lett. 12 (2012) 3507.
[12] A. Fleurence, R. Friedlein, T. Ozaki, H. Kawai, Y. Wang, Y. Yamada-Takamura, Phys. Rev. Lett. 108 (2012) 245502.
[13] L. Meng et al., Nano Lett. 13 (2013) 685.
[14] M.R. Tchalala et al., Appl. Phys. Lett. 102 (2013) 083107.
[15] A.K. Geim, I.V. Grigorieva, Nature 499 (2013) 419. and references therein.
[16] M.I. Katsnelson, K.S. Novoselov, A.K. Geim, Nat. Phys. 2 (2006) 620.
[17] S.B. Tang, J.P. Yu, L.X. Liu, Phys. Chem. Chem. Phys. 15 (2013) 5067.
[18] T.H. Wang, Y.F. Zhu, Q. Jiang, J. Phys. Chem. C 117 (2013) 12873.
[19] M. Housa, B. van den Broek, E. Scalise, G. Pourtois, V.V. Afanśev, A. Stesmans, Phys. Chem. Chem. Phys. 15 (2013) 3702.
[20] H.S. Liu, J.F. Gao, J. Zhao, J. Phys. Chem. C 117 (2013) 10353.
[21] N. Gao, J.C. Li, Q. Jiang, Chem. Phys. Lett. 592 (2014) 222.
[22] Y. Ding, Y.L. Wang, Appl. Phys. Lett. 103 (2013) 043114.
[23] T. Morishita, S.P. Pusso, I.K. Snook, M.J.S. Spencer, K. Nishio, M. Mikami, Phys. Rev. B 82 (2010) 045419.
[24] B. Huang et al., Phys. Rev. X 4 (2014) 021029.
[25] M. Houssa, G. Pourtois, V.V. Afanasév, A. Stesmans, Appl. Phys. Lett. 97 (11) (2010) 112106.
[26] H. Nakano et al., Angew. Chem. Int. Ed. 45 (2006) 6303.
[27] J.R. Dahn, B.M. Way, E. Fuller, Phys. Rev. B 48 (1993) 17872.
[28] S. Grimme, J. Comput. Chem. 27 (2007) 1787.
[29] B. Delley, J. Chem. Phys. 92 (1990) 508.
[30] B. Delley, J. Chem. Phys. 113 (2000) 7756.
[31] J.P. Perdew, K. Burke, M. Ernzerhof, Phys. Rev. Lett. 77 (1977) 3865.
[32] D.D. Koelling, B.N. Hartreermon, J. Phys. C: Solid State Phys. 10 (1977) 3107.
[33] J.P. Perdew, Y. Wang, Phys. Rev. B 45 (1992) 13244.
[34] W. Liu, J. Carrasco, B. Santra, A. Michaelides, M. Scheffler, A. Tkatchenko, Phys. Rev. B 86 (2012) 245405.
[35] W. Liu, S.N. Filimonov, J. Carrasco, A. Tkatchenko, Nat. Commun. 4 (2013) 2569.
[36] W. Liu, V.G. Ruiz, G.X. Zhang, B. Santra, X. Ren, M. Sheffler, A. Tkatchenko, New J. Phys. 15 (2013) 053046.
[37] A. Tkatchenko, M. Scheffler, Phys. Rev. Lett. 102 (2009) 073005.
[38] N. Gao, W.T. Zheng, Q. Jiang, Phys. Chem. Chem. Phys. 14 (2012) 257.
[39] W.J. Liu, I.D. Sharp, T.D. Tilley, Langmuir 30 (2014) 172.
[40] Y.F. Li, Z.F. Chen, J. Phys. Chem. Lett. 4 (2013) 269.
[41] Z.Y. Ni et al., Nano Lett. 12 (2012) 113.